HHS Public Access

Author manuscript

Free Radic Biol Med. Author manuscript; available in PMC 2023 July 11.

Published in final edited form as:

Free Radic Biol Med. 2022 November 20; 193(Pt 1): 274–291. doi:10.1016/j.freeradbiomed.2022.10.269.

Dynamics of Antioxidant Heme Oxygenase-1 and Pro-Oxidant p66Shc in Promoting Advanced Prostate Cancer Progression

Dannah R. Miller[1,#], **Matthew A. Ingersoll**[1,+], **Yu-Wei Chou**[1,++], **Elizabeth A. Kosmacek**[1], **Rebecca E. Oberley-Deegan**[1,2], **Ming-Fong Lin**[1,2,3,4,*]

[1]Department of Biochemistry and Molecular Biology, University of Nebraska Medical Center, Omaha, Nebraska, United States of America

[2]Fred and Pamela Buffett Cancer Center, University of Nebraska Medical Center, Omaha, Nebraska, United States of America

[3]Eppley Institute for Research in Cancer and Allied Diseases, University of Nebraska Medical Center, Omaha, Nebraska, United States of America

[4]Section of Urology, Department of Surgery, University of Nebraska Medical Center, Omaha, Nebraska, United States of America

Abstract

The castration-resistant (CR) prostate cancer (PCa) is lethal and is the second leading cause of cancer-related deaths in U.S. males. To develop effective treatments toward CR PCa, we investigated reactive oxygen species (ROS) signaling pathway for its role involving in CR PCa progression. ROS can regulate both cell growth and apoptosis: a moderate increase of ROS promotes proliferation; its substantial rise results in cell death. p66Shc protein can increase oxidant species production and its elevated level is associated with the androgen-independent (AI) phenotype of CR PCa cells; while heme oxygenase-1 (HO-1) is an antioxidant enzyme and elevated in a sub-group of metastatic PCa cells. In this study, our data revealed that HO-1 and p66Shc protein levels are co-elevated in various AI PCa cell lines as well as p66Shc cDNA-transfected cells. Knockdown and/or inhibition of either p66Shc or HO-1 protein leads to reduced tumorigenicity as well as a reduction of counterpart protein. Knockdown of HO-1 alone results in increased ROS levels, nucleotide and protein oxidation and induction of cell death. Together, our data indicate that elevated HO-1 protein levels protect PCa cells from otherwise apoptotic conditions induced by aberrant p66Shc/ROS production, which thereby promotes PCa progression to the CR phenotype. p66Shc and HO-1 can serve as functional targets for treating CR PCa.

[*]**Corresponding Author:** Ming-Fong Lin, Ph. D., Department of Biochemistry and Molecular Biology, College of Medicine, University of Nebraska Medical Center, 985870 Nebraska Medical Center, Omaha, NE 68198-5870, USA, TEL: (402) 559-6658, FAX: (402) 559-6650, mlin@unmc.edu (MFL).

[#]Present Address

SeaGen, Bothell, Washington, United States of America

[+]Present Address

Department of Pharmacology and Neuroscience, Creighton University, Omaha, Nebraska, United States of America

[++]Present Address

Drug Commercialization Center, Development Center for Biotechnology, Taipei, Taiwan

Declaration of interest

The authors declare no conflict of interest regarding the publication of this work.

Graphical Abstract

Hypothesis: Dynamic regulation of cellular ROS balanced by p66Shc and HO-1, leading to the progression of prostate cancer to the castration-resistant phenotype.

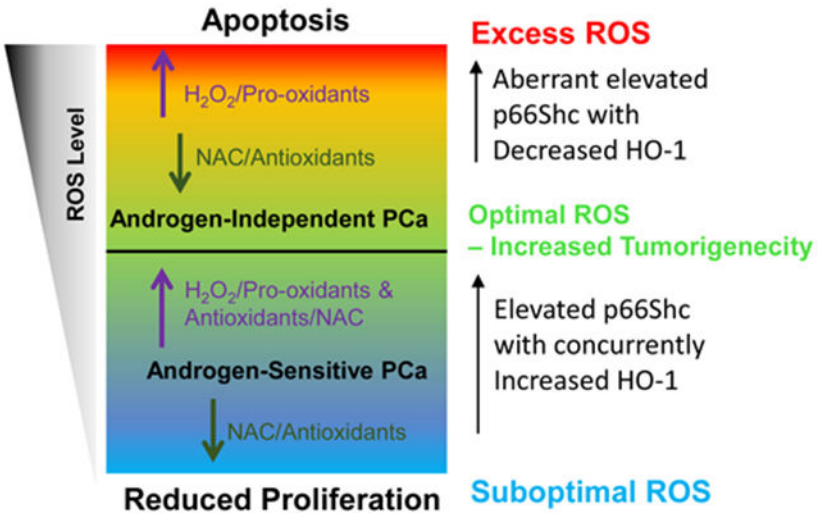

Keywords

Prostate Cancer; Castration-Resistant Prostate Cancer; Dynamic Redox Balance; HO-1; p66Shc; Heme Oxygenase-1; Reactive Oxygen Species

Introduction

Prostate cancer (PCa) is the most commonly diagnosed solid tumor and the second leading cause of cancer-related deaths in U.S. men [1]. Most metastatic PCa obtain the castration-resistant (CR) phenotype under androgen deprivation therapy (ADT) through various mechanisms [2-4] and currently, CR PCa has no effective or curative therapies [4-6]. Therefore, we are investigating the molecular mechanism of CR PCa progression to aid in the development of alternative therapies to treat this lethal disease.

Cellular reactive oxygen species (ROS) has been proposed to play a role in the progression of many types of cancers, including PCa [7]. Increased ROS levels in PCa are supported by the observations of elevated levels of oxidative damage markers, e.g., malondialdehyde and 8-oxoguanine, higher than that in benign prostate tissue [8,9]. Furthermore, an androgen-induced increase in ROS and oxidant species are shown to promote PCa cell proliferation, migration, invasion and metastasis [10-13] as well as augment mitochondrial activity [14-17].

p66Shc is a member of the Shc (Src homology-collagen homolog) adaptor protein family [18-20]. p66Shc can enhance oxidant species including superoxide production via two pathways: within the cytosol, p66Shc through Rac1 can interact with NOX enzymes to generate O_2^-; p66Shc can also localize to mitochondria and interact with cytochrome C to promote the leakage of electrons from the electron transport chain to form O_2^-. The function

of p66Shc in enhancing ROS production thus lends its role to a variety of cellular processes, e.g., longevity, senescence, cell proliferation and apoptosis, resulting in its role in aging and diseases [20-22]. In PCa, p66Shc protein levels are elevated in clinical adenocarcinomas compared to that of benign prostate tissues [11,23]. In androgen-sensitive (AS) PCa cells, androgen treatments increase p66Shc protein that leads to increased oxidant species production and cell proliferation, and p66Shc protein level is also higher in androgen-independent (AI) cells than in the corresponding AS cells [10-13,23]. Furthermore, elevated p66Shc protein levels by cDNA transfection supports AS cell proliferation and migration under steroid-reduced (SR) conditions in culture and tumor development in xenograft animals with low circulating androgens, a CR PCa phenotype [11-13]. Together, elevated p66Shc enhances PCa cell tumorigenecity and metastasis as well as obtains the CR phenotype in xenograft animals [11,13].

While increased ROS can enhance tumorigenicity, excessive ROS generation results in cytotoxicity, including oxidative damage of nucleotides, proteins, and lipids, leading to apoptosis. Cancer cells are known to be in a pro-oxidant state for progression, therefore they often develop mechanisms to protect themselves against toxic levels of ROS, in part by expressing a set of cytoprotective molecules to prevent from apoptosis. Heme oxygenase-1 (HO-1) is such a protein that is involved in the degradation of heme, an inflammatory agent [26,27]. HO-1 is the rate-limiting enzyme of heme degradation to free iron, carbon monoxide and biliverdin that is rapidly converted to the antioxidant bilirubin by biliverdin reductase. Both biliverdin and bilirubin can react with O_2^- to reduce levels of this toxic ROS species. Under physiological conditions, HO-1 expression is quite low. However, HO-1 expression and activity can be stimulated for several folds by various factors, including heme, ROS (particularly O_2^-), UV irradiation, physical stress, cytokines, and growth factors [28]. HO-1 is shown to be associated with tumor growth, aggressiveness, metastatic potential, drug resistance, and/or poor prognosis in a variety of cancers [29]. In PCa, while there is little to no detection of HO-1 in AS PCa or benign tissue, HO-1 protein level is significantly elevated in a subgroup of metastatic PCa archival specimens, particularly that of hormone-refractory/CR PCa [30-33]. Nevertheless, the regulation of HO-1 elevation in PCa cells and its function of counterbalancing with pro-oxidant production remain further investigation.

In this study, we discovered a pair of redox proteins: one prooxidant protein and its corresponding antioxidant protein; together they maintain a high level of ROS for supporting CR PCa progression without allowing the ROS balance to reach toxic levels. We found that in PCa cells, an increase or decrease of p66Shc protein correlates with respective increase or reduction of HO-1 protein and its potent inducer heme levels. Conversely, knockdown HO-1 leads to increased cellular ROS levels and nucleotide and protein oxidation as well as the induction of cell death particularly in SR conditions. Further, treatment of p66Shc-elevated PCa cells with HO-1 competitive inhibitor zinc protoporphyrin IX (ZnPPIX) in combination with radiation led to enhanced anti-tumor activity. Hence, elevated HO-1 protects PCa cells from aberrantly excessive p66Shc-induced ROS and preventing them from oxidative damage, concurrently, those cells maintain a high level of ROS resulting in promoting advanced CR PCa progression. p66Shc and HO-1 together can serve as functional targets for developing an effective treatment for CR PCa.

Materials and Methods

Materials

RPMI 1640 medium, DMEM medium, Keratinocyte SFM medium, gentamicin, and L-glutamine were obtained from Invitrogen (Carlsbad, CA). HPC1 medium was purchased from Fischer Scientific (Pittsburgh, PA, USA). Fetal bovine serum (FBS) and charcoal-treated FBS (cFBS) were purchased from Atlanta Biologicals (Lawrenceville, GA). Heme Oxygenase-1 siRNA and siTran 1.0 were purchased from Origene (Rockville, MD). Protein molecular weight standard markers, acrylamide, and Bradford protein assay kit were purchased from Bio-Rad (Hercules, CA). Anti-AR (5153S, 1:2000), anti-Caspase 3 (9662S, 1:2000), anti-PARP (9532S, 1:2000), anti-cyclin B1 (#4135S, 1:1000), and anti-Keap-1 (#8047, 1:1000) were purchased from Cell Signaling Technology (Beverly, MA, USA). Anti-NFκB (sc-372, 1:1000), anti-Bcl_{XL} (sc-8392, 1:1000), anti-Bax (sc-6236, 1:1000), anti-PCNA (sc-56, 1:1000), cytosolic PSA (sc-7638, 1:1000), Cyclin D1 (sc-718, 1:1000), prostatic acid phosphatase (PAcP) (sc-80908, 1:1000), Survivin (sc-8807, 1:1000), and horseradish peroxidase-conjugated anti-mouse (#C2011, 1:5000), and anti-rabbit (#D2910, 1:5000) IgG antibodies (Abs) were all acquired from Santa Cruz Biotechnology (Santa Cruz, CA). Anti-Nrf2 (ab62352, 1:1000), anti-carbonyl (ab178020, 1:1000), and DNA/RNA Damage (8OHG) (ab62623, 1:1000) Abs was purchased from Abcam. Anti-Catalase (#AF3398, 1:2000) Abs and Peroxy Orange-1 (PO-1) were obtained from R&D Systems (Minneapolis, MN). Anti-Shc (#06-203, 1:5000) and phosphor-Shc (#07-209, 1:1000) Abs were obtained from Upstate Biotech. Inc. (Lake Placid, NY). Anti-Superoxide Dismutase-1 (SOD1) (1:2000) and anti-SOD2 (1:2000) Abs were a generous gift from Fredrick Domann. Anti-HO-1 (ADI-OSA-110-F, 1:1000) and Cysteine (sulfonate) (ADI-OSA-820-D, 1:1000) Abs were purchased from Enzo Biologicals. Anti-β-Actin (#99H4842, 1:10000) Ab, N-acetyl cysteine (NAC), hydrogen peroxide (H_2O_2), and MitoTracker were procured from Sigma (St. Louis, MO). DAPI Hard-Mount Medium was obtained from Vector Laboratories (Burlingame, CA). Nitro-blue tetrazolium (NBT), riboflavin-5-phosphate, MG132, and Lactacystin were purchased from Sigma-Aldrich (Darmstadt, Germany).

Cell Culture

Human prostate cancer cell lines LNCaP, MDA PCa2b and VCaP were originally purchased from the American Type Culture Collection (Rockville, MD) and cultured according to the accompanied protocols and our publications [34-36]. LNCaP cells were maintained in RPMI medium containing 5% FBS, 2 mM glutamine and 50 μg/ml gentamicin. MDA PCa2b cells were maintained in HPC1 medium containing 20% FBS, 2nM glutamine and 50 μg/ml gentamicin. VCaP cells were maintained in DMEM medium containing 15% FBS, 2 mM glutamine, 50 μg/ml gentamicin and 10 μg/ml ciprofloxacin. To mimic conditions of clinical ADT, cells were maintained in SR conditions, i.e., phenol red-free RPMI 1640 medium containing 5% charcoal-stripped FBS, 2 mM glutamine, 50 μg/ml gentamicin and 1 nM [34-38].

AI LNCaP C-81 cells were established per our publications [34-36]. LNCaP C-81 cells exhibit many biochemical properties similar to CR PCa, including cell proliferation and PSA secretion in SR conditions, and importantly, obtaining the intracrine biosynthesis of

endogenous testosterone from cholesterol with activated AR [3]. Within this manuscript to be consistent with the other AI cells, AI LNCaP C-81 cells are abbreviated as LNCaP-AI cells. Similarly, we established MDA PCa2b-AI and VCaP-AI cells that obtained the AI phenotype, including rapid cell proliferation in SR media [37,38]

Transfection

For transient transfection experiments, LNCaP cells were plated at a density of $1x10^4$ cells per cm2 and transfected using Lipofectamine and Plus reagents or siTran 1.0. Five hours after transfection, cells were fed with RPMI media containing 10% FBS for 24 hrs. The cells were then used for trypan blue exclusion, clonogenic, and transwell assays, immunofluorescence, and harvesting whole cell lysates for immunoblot analysis. Stable subclones of LNCaP cells transfected with p66Shc wildtype (WT) cDNA were established as described previously [11,17,25]. For knockdown of p66Shc expression, transient transfection of pSUP-p66 plasmid-based small interfering RNA system targeted against the CH2 domain was used for transfection as described previously [25]. Competitive inhibition of p66Shc-enhanced ROS production activity was achieved upon transfection of cells with p66Shc W134F redox-impaired mutant cDNA [12]. For knockdown of HO-1, HO-1-targeted siRNA was purchased and utilized per company instructions (Origene).

Superoxide Dismutase Activity Assay

For analysis of SOD activity, cells were washed with HEPES buffered saline, pH 7.0, harvested by scraping, and lysed in ice-cold lysis buffer. Protein concentrations of the supernatant were determined using Bio-Rad Bradford protein-assay. An aliquot of the total cell lysate was electrophoresed on a 10% native gel at 70 mA for 3 h at 4°C. Gels were then incubated in 2.5 mM NBT in the dark at room temperature for 20 minutes, then incubated with 5 nM riboflavin-5-phosphate in 36 mM phosphate buffer, pH 7.8, plus TEMED on a light box for 20 minutes. Gels were then washed with water until the gel turned dark purple.

Metabolite Analysis

Cell pellets were prepared from LNCaP-AS, LNCaP-AI, MDA PCa2b-AS, MDA PCa2b-AI, and p66Shc cDNA-transfected stable subclones of LNCaP-AS cells. The cell pellets were frozen by dry ice and sent to METABOLON Inc. (Durham, NC) for analysis of the levels of 297 metabolites (Contract: UNNE-01-11VW). The data were quantified and analyzed by the company. Values were normalized in terms of raw area counts (OrigScale). For a single day run, this is equivalent to the raw data. Each biochemical in OrigScale is rescaled to set the median equal to 1 and expressed as imputed normalized counts for each biochemical (ScaledImpData).

Cell Proliferation by Trypan Blue Dye Exclusion Assay

To determine the effects of the compounds on PCa cell growth, LNCaP-AI and p66Shc subclone cells were plated at 2×10^4 cells per well in 6-well plates for 72 hours. Cells were then transfected with 10 nM of control or HO-1 siRNA or Control or p66Shc shRNA or treated with ZnPPIX as described in the figure legends in FBS or SR medium for 72 hours.

The cell number was counted by a cell counter cellometer™ Auto T4 (Nexcelom Bioscience, USA) using trypan blue dye exclusion assay [38-40].

Immunofluorescence

Experimental cells were plated at 5 x 10^4 cells per well in 12-well plate on autoclaved round coverslips in FBS medium and allowed to attach for 24 hours. Cells were treated as indicated in the text and then fixed in 4% paraformaldehyde in phosphate buffered saline (PBS) for 10 min at room temperature. Cells were rinsed three times in PBS. The cells were then incubated with primary antibody in PBS containing 0.5% BSA for 1 h at room temperature, washed three times in PBS and then incubated with the appropriate fluorochrome-conjugated secondary antibodies diluted in PBS containing 0.5% BSA for 30 min. Cells were washed three times in PBS and mounted in Fluoromount. Using a Zeiss LSM 800 confocal microscope with a 63x/1.4 NA oil objective, confocal images were collected. ImageJ was used for fluorescence quantification [12,40].

ROS Level Determination

LNCaP-AI and p66Shc subclone cells were plated at 5 x 10^4 cells per flask in FBS medium and allowed to attach for 24 hours. Cells were then transfected with 10 nM of control or HO-1 siRNA for 72 hours in FBS medium, then washed with PBS. To analyze cells for cellular levels of total ROS, cells were stained with 20 μM DCF-DA in the dark for 30 minutes before being washed with PBS and examined via a Becton-Dickinson fluorescence-activated cell sorter (FACSCalibur, Becton Dickinson, San Jose, CA, USA) at the UNMC Flow Cytometry Core Facility [12,40].

Immunoblot Analysis

For immunoblot analyses, cells were washed with HEPES buffered saline, pH 7.0, harvested by scraping and lysed in ice-cold lysis buffer containing protease and phosphatase inhibitors [12,38-40] . Protein concentrations of the cell lysates were determined using Bio-Rad Bradford protein-assay. An aliquot of the total cell lysate was electrophoresed on SDS-polyacrylamide gels (7.5%-12%). After transfer to a nitrocellulose membrane, the membranes were blocked with 5% non-fat milk in Tris-buffered saline (TBS) containing 0.1% Tween-20 for 60 minutes at room temperature. Membranes were incubated with the corresponding primary antibody at 4°C overnight. Membranes were rinsed with TBS and incubated with the proper secondary antibody for 60 minutes at room temperature. Proteins were detected using enhanced chemiluminescence (ECL) reagent kit. β-actin was used as a loading control [12,38-40].

Statistical Analysis

Each set of experiments was conducted in triplicate or quadruplicate as specified in the figure legends, and experiments were repeated independently at least three times (i.e., 3x3 or 4x3). The mean and standard error values of results were calculated, and two-tailed student-t-test via Microsoft Excel was used to determine the significance of results. $p<0.05$ was considered statistically significant. Quantification of Western blot bands was performed on the program Image-J before undergoing statistical analysis.

Results

Effects of ROS on the Proliferation of AS vs. AI PCa cells

Since the levels of oxidative stress markers are elevated in PCa cells, ROS is proposed to play a role in clinical PCa progression [8,14]. We investigated the role of ROS in promoting CR PCa progression by analyzing the effects of oxidant H_2O_2 *vs.* antioxidant NAC on the proliferation of LNCaP-AS cells in steroid-reduced conditions, mimicking androgen-deprivation conditions. As shown in Fig. 1A, H_2O_2 treatments increased cell growth following a dosage response in which 5 μM of H_2O_2 could promote a significant cell growth ($p<0.05$) with 10 μM being the optimal effect. Conversely, antioxidant NAC treatment significantly reduced both the basal cell growth as well as counteracted H_2O_2-stimulated cell proliferation (Fig. 1A).

Treatment of LNCaP-AS PCa cells with H_2O_2 (10 μM) exhibited the optimal growth stimulation in SR conditions (Fig. 1A), therefore this concentration of H_2O_2 was thus utilized throughout the rest of the study. 10 μM H_2O_2 treatment increased MDA PCa2b-AS cell growth by about 80%; and 10 mM NAC treatment reduced the basal growth of MDA PCa2b-AS cells by 50% (Fig. 1B). NAC abolished the stimulatory effect of concurrent H_2O_2 treatment on the proliferation in MDA PCa2b-AS cells (Fig. 1B). A similar trend was seen in VCaP-AS cells in which H_2O_2 treatment increased basal cell proliferation, while NAC treatment effectively reduced both basal and H_2O_2-stimulated cell proliferation (Fig. 1C). Hence, under steroid-reduced conditions, oxidants increase AS PCa cell proliferation which is counteracted by antioxidants.

We analyzed ROS *vs.* NAC effects on PCa-AI cells that exhibit higher ROS levels than the corresponding AS cells by 2-3 fold [11,13]. AI PCa cells, including LNCaP-AI, MDA PCa2b-AI and VCaP-AI cells, were treated with H_2O_2 with/without NAC, similarly to AS PCa cell treatments. 10 μM H_2O_2 treatments resulted in a 55-60% reduction in the proliferation of LNCaP-AI, MDA PCa2b-AI, and VCaP-AI cells, while 10 mM NAC treatment increased proliferation by about 40%; the concurrent treatment of H_2O_2 and NAC resulted in no significant effect on cell proliferation of all three AI PCa cells (Fig. 1D-1F). Hence, oxidants and antioxidants exhibit opposite effects on cell proliferation in AS vs. AI PCa cells in SR conditions.

We analyzed cellular H_2O_2 levels via Peroxy Orange-1 (PO-1) staining in LNCaP-AS and -AI cells. Figure 1G showed that LNCaP-AI cells exhibit 2-3-fold higher basal levels of H_2O_2 than corresponding LNCaP-AS cells. Further, treatments of LNCaP-AS and AI with H_2O_2 or NAC resulted in a corresponding increase or decrease in cellular H_2O_2 levels, respectively, and concurrent treatment with both H_2O_2 and NAC mitigated the effects of either compound on cellular H_2O_2 levels. The data collectively demonstrates a balance of ROS levels in regulating PCa cell proliferation.

HO-1 and p66Shc are Co-Elevated in AI PCa Cells

Pro-oxidant protein p66Shc level is elevated in clinical PCa samples and AI PCa cells, higher than respective controls, and plays a role in up-regulating AI PCa proliferation and migration [11-13, 17,23]. Hence, we analyzed the redox protein profiles of AS versus

respective AI PCa cells to determine if there is a corresponding antioxidant response to an elevation of p66Shc protein levels. Western blot analyses clearly showed that among 3 PCa cell progressive models, p66Shc protein level, but not p52Shc or p46Shc, is consistently elevated in AI cells, higher than that in the corresponding AS cells, as seen in p66Shc cDNA-transfected subclone cells (Figure 2A). Further, there is no significant change in protein levels of catalase and SOD2 (Figure 2A) in all p66Shc-elevated LNCaP-AI, MDAPCa2b-AI and VCaP-AI PCa cells as well as p66Shc subclone cells, compared to their AS counterparts. SOD1 protein level was elevated in VCaP-AI and p66Shc subclones compared to VCaP-AS and V1 cells, respectively; however, there was no significant change in SOD1 protein levels in LNCaP-AI or MDA PCa2b-AI cells compared to their respective AS cells. Analysis of SOD activity revealed that SOD activity essentially correlated with its protein level except SOD1 activity in VCaP-AI cells, and there was no significant alteration in SOD1 or SOD2 activity in AI PCa cells compared to their AS counterparts (Fig. 2A).

Further analyses revealed that there is a consistent increase in protein levels of Nrf2 and a reduction in its negative regulator Keap1 in AI PCa cells except Keap1 in p66Shc subclones. Additionally, Nrf2 localization to the nucleus was increased in LNCaP-AI and p66Shc subclones compared to LNCaP-AS and V1 cells, respectively (Fig. S1). Interestingly, the protein level of Nrf2-downstream target HO-1 was highly elevated, correlating with increased p66Shc protein in all AI PCa and p66Shc subclone cells (Fig. 2A). Metabolomic analyses revealed a significant increase in heme levels, a potent inducer of HO-1 expression and activity, in AI PCa cells and p66Shc subclones compared to AS PCa cells (Fig. 2B). Heme levels were increased by average 50% in LNCaP-AI and p66Shc subclones compared to LNCaP-AS cells, while MDA PCa2b-AI cells had about 200% increase in heme levels over MDA PCa2b-AS cells. Together, the data shows a strong association between pro-oxidant p66Shc and antioxidant HO-1, but not Catalase, SOD1/2 or NFκB (data not shown), implicating that the co-elevation of p66Shc and HO-1 proteins is vital for PCa progression to the AI phenotype.

Nrf2 and HO-1 Protein Levels and PCa Cell Proliferation are Reduced upon Decreased p66Shc Protein or Activity

To determine the relationship between pro-oxidant p66Shc protein and antioxidant HO-1 protein, which relates to cell proliferation, we knocked down p66Shc expression in LNCaP-AI cells and p66Shc subclones by transfecting with p66Shc shRNA vector. In p66Shc shRNA-transfected cells, p66Shc, Nrf2 and HO-1 protein levels decreased, following the increased amount of p66Shc shRNA (Fig. 3A and 3C). Nrf2 peri-nuclear localization was also reduced in p66Shc-knockdown LNCaP-AI cells and p66Shc subclones (Fig. S1). Significantly, the growth of p66Shc shRNA-transfected LNCaP-AI cells and p66Shc subclones was decreased, following a dose-dependent fashion (Fig. 3B and 3D).

We analyzed whether the changes of these phenotypes were due to ROS produced via p66Shc enhancement, cells were transfected with cDNA encoding the p66Shc W134F redox-impaired mutant with no pro-oxidant activity. The p66Shc mutant competitively inhibits the wild type p66Shc pro-oxidant activity [12,17,41]. Similar results were seen in both p66Shc W134F redox-impaired mutant-transfected LNCaP-AI cells and p66Shc

subclones in which Nrf2 and HO-1 protein levels were reduced (Fig. 3E and 3G) as well as a dose-dependent decrease in cell proliferation (Fig. 3F and 3H). Together, the data show the association between HO-1 protein level and ROS production with p66Shc protein, and further support the role of p66Shc via ROS in enhancing PCa cell proliferation [12,13,17].

p66Shc Protein and PCa Cell Proliferation is Reduced upon HO-1 Inhibition or Knockdown

Since preliminary data showed the treatment with HO-1 competitive inhibitor ZnPPIX led to a reduction in p66Shc protein levels and proliferation of LNCaP-AI cells (data not shown), we further determined the interactive relationship between HO-1 and p66Shc and their effects on cell proliferation by inhibiting HO-1 activity via HO-1-targeted siRNA. Knockdown of HO-1 by siRNA in LNCaP-AI cells resulted in decreased p66Shc protein levels and cell proliferation in both regular media containing FBS and SR conditions containing cFBS (Fig. 4A). Consistently, Fig. 4B and 4C showed that knockdown of HO-1 in p66Shc subclones resulted in significantly reduced cell proliferation in both growth conditions.

Figure S2 shows that upon transfection with HO-1 siRNA, both cell migration and colony formation of LNCaP-AI and p66Shc subclones were reduced. Migration was reduced in LNCaP-AI cells by about 35% in FBS conditions while it was reduced by 50% in SR conditions (Fig. S2A). In p66Shc subclones, migration was reduced by 60% in both FBS and SR conditions (Figs. S2B and S2C). Similarly, there were significantly fewer colonies in HO-1 siRNA-transfected LNCaP-AI cells in SR conditions at about an 85% reduction in colony formation compared to a 60% decrease in FBS conditions (Fig. S2D). This was also a drastic effect on p66Shc subclones by siRNA to HO-1, which resulted in about an 85% reduction in colony formation in FBS conditions and a 90% reduction in SR conditions (Figs. S2E and S2F). Interestingly, AS V1 cells had about 50-60% reduction in migration or colony formation upon knockdown of HO-1 in both FBS and SR conditions (Fig. S2).

Visualization under a confocal microscope further confirmed that p66Shc protein levels are reduced by about 50% upon transfection with HO-1 siRNA or p66Shc shRNA in LNCaP-AI cells. p66Shc localization to the mitochondria was also reduced when p66Shc levels were reduced by about 60% upon HO-1 or p66Shc knockdown (Fig. S3A). Knockdown of HO-1 or p66Shc in p66Shc subclones also resulted in reduced p66Shc protein levels by 35% and 90%, respectively, as well as reduced p66Shc localization to the mitochondria (Fig. S3B).

We analyzed effect of HO-1 knockdown on the stability of p66Shc protein. Control and HO-1 siRNA transfected LNCaP-AI cells were treated with ubiquitin inhibitors MG132 and Lactacystin, and cell lysates were then analyzed for p66Shc and HO-1 protein levels. Both MG132 and Lactacystin treatments prevented the reduction of p66Shc protein levels seen in HO-1 siRNA transfected cells. Interestingly, there were higher HO-1 protein levels upon Lactacystin treatment, indicating this is the main pathway of HO-1 degradation (Fig. S3C). Thus, these data demonstrate that the knockdown of HO-1 promotes p66Shc degradation and reduces the amount of p66Shc protein localized to the mitochondria.

Reduced HO-1 Protein Increases Cellular Oxidative Environment and Increases SOD1 Activity

To investigate the effect of HO-1 expression on oxidative stress, we semi-quantified cellular ROS and H_2O_2 levels. Figure 5A (Left panel) showed that by DCF-DA analyses, upon knockdown of HO-1 by siRNA in LNCaP-AI cells, total cellular ROS was significantly increased by about 25% compared to control siRNA-transfected cells. Further, there was about 30% higher basal levels of ROS in p66Shc subclones compared to V1 cells (Right panel, Fig. 5A). Upon knockdown HO-1 by siRNA, total ROS in V1 cells was increased by about 30%, while p66Shc subclones had an over 70% increase in ROS (Fig. 5A, Right panel). Analyses of cellular H_2O_2 levels via Peroxy Orange-1 (PO-1) staining showed that there is about 160% increase in PO-1 staining in HO-1 siRNA-transfected LNCaP-AI cells compared to cells transfected with control siRNA (Fig. 5B). Significantly, p66Shc subclones had about twice as much PO-1 staining at basal levels compared to V1 cells. Upon HO-1 siRNA transfection, while there was no quantifiable change in PO-1 staining in V1 cells, there was an increase by over 50% in p66Shc subclones upon knockdown of HO-1 compared to its own control cells (Fig. 5B).

To investigate if there is a compensatory effect on other antioxidant protein in HO-1-knockdown cells, we analyzed antioxidant proteins Nrf2, SOD1, SOD2 and catalase via Western blotting. Upon HO-1 siRNA transfection, SOD1 protein levels, but not SOD2 protein, were elevated in LNCaP-AI and p66Shc subclone cells (Fig. 6). Similarly, in HO-1 knockdown cells, SOD1 activity was increased but not SOD2 activity (Fig. 6). Interestingly, catalase protein level was increased in HO-1 siRNA-transfected V1 and p66Shc subclone cells, but not in LNCaP-AI cells (Fig. 6). Upon knockdown of HO-1, there is a reduction in Nrf2 protein levels (Fig. 6) as well as Nrf2 localization to the nucleus (Fig. S1). Thus, in HO-1 knockdown cells, while antioxidant SOD1 activity is activated (Fig. 6), cellular ROS levels still increased (Fig. 5), indicating the critical importance of HO-1 as the key antioxidant protein in p66Shc-elevated PCa cells.

HO-1 Protects AI PCa Cells from Oxidative Damage and Cell Death

Increased cellular ROS levels can oxidize vital molecules within the cell [Ma 2018]; therefore, we analyzed nucleotide and protein oxidation levels upon knockdown of HO-1. Figure 7A showed that LNCaP-AI cells experienced an increased nucleotide oxidation about 190% increase in 8OHG by an anti-8OHG antibody upon transfection of HO-1 siRNA. Similarly, p66Shc subclones, but not its V1 control cells, had about 100% increase in nucleotide oxidation upon HO-1 knockdown (Fig. 7A). A similar pattern was seen upon detection of oxidized cysteine residues in which HO-1 knockdown resulted in about 70% increase in staining in LNCaP-AI cells and about 50% increase in p66Shc subclones, while there was no significant alteration of oxidized cysteine residues in V1 cells (Fig.7B). Similarly, increased protein carbonylation was also detected upon knockdown of HO-1 in LNCaP-AI, V1, and p66Shc subclone cells via Western blot analyses (Fig. 7C). Together, the data demonstrate that HO-1 plays a critical role in protecting AI PCa cells from excessive nucleotide and protein oxidation by aberrant elevated p66Shc/ROS.

We analyzed the alteration of cell signaling in survival and growth regulation upon HO-1 knockdown via Western blot analyses. LNCaP-AI, V1, and p66Shc subclone cells were transfected with Control or HO-1 siRNA in both regular-FBS and SR-cFBS conditions, and cell lysates were analyzed for proliferative and apoptotic proteins. Figs. 8A and 8B clearly show that upon HO-1 siRNA transfection, while androgen receptor (AR) protein level was not consistently altered in cells, there was a dramatic reduction of AR-regulated cytosolic PSA (cPSA) levels in all transfected cells under both regular-FBS and SR-cFBS conditions. Cell proliferation markers Cyclin B1 and PCNA as well as Nrf2 were reduced in HO-1-knockdown cells in both conditions, except PCNA in V1 cells in FBS condition. Analyses of apoptotic markers revealed that upon transfection with HO-1 siRNA, there was an increase in pro-apoptotic Bax while its anti-apoptotic partner Bcl_{XL} was reduced. Consistently, apoptotic proteins Cleaved Caspase 3 and Cleaved PARP levels in HO-1 siRNA-transfected cells were increased except that in V1 cells having low p66Shc/ROS levels (Figs. 8A&8B).

Cell cycle analyses at 48 hours post-transfection of HO-1 siRNA revealed that while there was no alteration in G1/G0, S or G2/M phases in LNCaP-AI, V1, or p66Shc subclone cells transfected with HO-1 siRNA in regular-FBS conditions, there was a significant increase in G2/M phase and reduction in G1/G0 phase upon transfection of LNCaP-AI with HO-1 siRNA in SR-cFBS conditions. Importantly, there was a significant increase in apoptotic cells detected in LNCaP-AI cells and p66Shc subclones upon knockdown of HO-1 (Fig. 8C). Furthermore, staining with early apoptosis detector YO-PRO-1 and late apoptosis stain propidium idiode (PI) demonstrated that there was an increase in both YO-PRO-1 and PI staining upon HO-1 knockdown in both regular-FBS and SR-cFBS conditions, with a greater increase in SR conditions (Fig. 8D). Together, these data suggest that HO-1 is critical for the survival of p66Shc-elevated PCa cells, especially in SR-cFBS conditions.

Combination Treatments with HO-1 Inhibitor ZnPPIX

To determine if the utilization of HO-1 competitive inhibitor ZnPPIX could be beneficial in combination with current PCa therapeutic options, we treated LNCaP-AI and p66Shc subclones with ZnPPIX in combination with abiraterone acetate (AA), docetaxel or radiation. Fig. 9A showed that ZnPPIX, AA, and the combination of these inhibitors led to a 25-30% reduction in cell proliferation. Further, 1 nM docetaxel reduced growth by about 40% while combination of docetaxel and ZnPPIX reduced growth by about 50%. Radiation alone reduced growth by about 35%, and the combination of radiation and ZnPPIX effectively reduced LNCaP-AI proliferation by 80% (Fig. 9A). Upon treatment of p66Shc subclone cells with ZnPPIX, there was a reduction in proliferation by 40%. 5 Gy radiation reduced proliferation by 20%, while the combination of radiation and ZnPPIX reduced proliferation in p66Shc subclones by 70% (Fig. 9B). These data demonstrate the enhanced anti-proliferative effects of the combination of ZnPPIX and radiation in PCa cells.

Discussion

CR PCa is a lethal disease of which patients succumb shortly upon development, thus understanding the mechanism of PCa progression from the AS to the AI phenotype is crucial

to developing therapeutic options for this patient population. In this study, we analyzed the effects of a novel redox protein pair, pro-oxidant p66Shc and antioxidant HO-1, which enhance PCa progression toward the CR phenotype. We also determined the protective role of HO-1 in AI PCa cells from excessive ROS production mediated by p66Shc.

We first analyzed the effects of ROS treatment on AS and AI PCa cell lines, including LNCaP, MDA PCa2b and VCaP cells. Interestingly, there is an increase in cell growth upon treatment of AS PCa cells with 10 μM H_2O_2, while AI PCa cells having 2-3-fold higher basal levels of ROS experienced reduced cell proliferation and cell death with same concentration of H_2O_2 (Fig. 1) [11]. Analyses on the redox signaling profile of those PCa cell lines as well as vector-alone transfected V1 cells compared to p66Shc cDNA-transfected subclones, demonstrated that p66Shc was increased in all AI PCa cells examined as well as p66Shc subclones, higher than the corresponding AS cells. Nrf2 and HO-1 were also consistently upregulated in p66Shc-elevated AI PCa cells and p66Shc subclones, while SOD protein levels and activities were not significantly altered (Fig. 2). Hence, we propose that HO-1 is the vital antioxidant counterpart to p66Shc, which is also indicated by observations in other cell types including hepatic cells and renal cells that the elevation of HO-1 in response to increased p66Shc can reduce oxidative damage in those cells [42,43]. The importance of HO-1 in p66Shc-elevated cells is further supported by metabolomic analyses, which revealed that heme, an inducer of HO-1 protein and activity, was also increased in LNCaP-AI and MDA PCa2b-AI cells and p66Shc subclones compared to their AS counterparts, all of which have increased p66Shc protein levels (Fig. 2B).

Upon p66Shc knockdown via transfection with p66Shc shRNA, Nrf2 and HO-1 protein levels were reduced in LNCaP-AI cells and p66Shc subclones. Transfection of cells with p66Shc W134F, a redox inactive mutant cDNA, also reduced Nrf2 and HO-1 protein levels. Biologically, transfection of either p66Shc shRNA or W134F cDNA reduced PCa cell proliferation (Fig. 3). We thus propose that while HO-1 and p66Shc are independently regulated, they are, at least in part, dynamically interconnected with each other via ROS levels, which leads to maintain an optimal ROS level for the proliferation of AI cells (Fig. 10). For comparison, knockdown of p66Shc in AS PCa cells those exhibit low levels of p66Shc protein resulted in no significant alteration of biological effects or altered HO-1 or Nrf2 protein levels (data not shown). Hence, elevated p66Shc via ROS production supports AI PCa cell proliferation [11-13]. The reduction of HO-1 levels upon p66Shc knockdown or inactivation by dominant negative mutant (Fig. 3) is a result of the reduction of ROS levels, which ultimately lead to a reduction in proliferation via ErbB-2 signaling [13].

Interestingly, HO-1 inhibition and knockdown reduces the tumorigenicity of LNCaP-AI cells and p66Shc subclones, more dramatically in SR conditions (Fig. 4), which suggests that HO-1 is a vital molecule in the maintenance of CR PCa, particularly those AI PCa cells driven by elevated p66Shc and/or increased ROS levels. It should also be noted that O_2^- and H_2O_2 often exhibit different effects on cell signaling [44], however, there are similar alterations in cell growth in AI cells when ROS is elevated via introduction of H_2O_2 (Fig. 1) or the loss of HO-1 protein or activity (Fig. 4), i.e., a reduction of O_2^- scavenging. The reduction of HO-1 protein levels or inhibition of its activity leads to a reduction in p66Shc protein as well (Fig. 4, Fig. S3C), thus suggesting its role as a counterbalance of p66Shc to

prevent aberrant ROS-induced cell death. Furthermore, p66Shc degradation can be at least in part in response to the increased ROS due to knockdown of HO-1 (Fig. S3C). Interestingly, in a study by Miyazawa et al., treatment of cells with HO-1 activator hemin increased p66Shc protein levels [45], further confirming the correlative relationship between these two proteins. Our results clearly demonstrate the novel dynamic balance of co-elevation between HO-1 and p66Shc; conversely, knockdown of one molecule results in the reduction the other.

It should be noted that our studies confirmed the critical antioxidant role of HO-1 in AI PCa cells, as HO-1 knockdown increases cellular ROS levels (Fig. 5). While most antioxidant proteins had minimal differences in protein and activity levels between AS and AI PCa cells (Fig 2), there is a potential for one or more of these proteins to be elevated upon loss of HO-1. It was determined that in attempt to compensate for the loss of vital antioxidant HO-1, cytoplasmic SOD1 levels and activity were increased, but not other antioxidant proteins analyzed (Fig. 6). Nevertheless, in those cells, cellular ROS levels still increased, which was accompanied by a significant increase in cell death (Fig 8) despite the attempt of SOD1 to compensate for the knockdown of HO-1. The data indicates that HO-1 is a vital antioxidant system in LNCaP-AI cells and p66Shc subclones. Although SOD1 is slightly upregulated and p66Shc is reduced upon knockdown of HO-1, these events are not sufficient to protect cells from nucleotide and protein oxidative damage (Fig. 7) or cell death, particularly in p66Shc-elevated cells under SR conditions (Fig 8), further validating the crucial role of HO-1 in p66Shc/ROS-elevated CR PCa survival. Interestingly, inhibition of HO-1 via ZnPPIX in combination with radiation may be an effective therapeutic option to treat clinical CR PCa (Fig. 9). Its further study is warranted.

Our results of HO-1 counter-balancing ROS by p66Shc in supporting of AI cell proliferation are consistent with those reports on the influence of HO-1 on CR PCa growth and metastasis *in vivo* xenograft animals. Elevated p66Shc supports AI PCa cell growth and metastasis in xenograft animals [13]. PC-3 cells express high levels of p66Shc [25] and HO-1 [46]. HO-1 shRNA transfection of PC-3 cells resulted in reduced tumor growth as well as lymph node and tumor metastasis *in vivo*. Similarly, CR PCa tumor growth and metastasis were also reduced upon treatment with HO-1 inhibitor OB-24, which had an additive anti-proliferative effect when combined with paclitaxel [31]. Importantly, ZnPPIX treatment has effective anti-tumor activity in a variety of cancers [47-50] and daily administration of this molecule does not demonstrate any apparent side effects in mice [51], thereby providing a potential therapeutic option for CR PCa.

Our data indicate that elevated HO-1 protein levels protect PCa cells from otherwise apoptotic conditions induced by aberrant p66Shc/ROS production, and thereby promotes AI PCa proliferation and migration as well as progression to the CR phenotype. This working hypothesis is demonstrated in Figure 10. Briefly, p66Shc enhances ROS generation via interaction with cytochrome c in the mitochondria or via activation of NOXs in the cytoplasm. Interestingly, increased ROS can also reduce p66Shc protein levels. Upon increased ROS levels, Nrf2 is activated and promotes transcription of antioxidant enzyme HO-1 to reduce ROS-induced oxidative stress and/or damage. (i) A substantial, excessive increase of ROS leads to cytotoxicity and apoptosis of the cell. (ii) However, a moderate

increase in ROS can promote PCa cell growth and survival via oxidation of growth factor receptor negative regulators, such as protein tyrosine phosphatases [11,25,52].

This study clearly showed the pro-tumorigenic effects of p66Shc protein on PCa cells as well as the impacts of HO-1 in preventing aberrantly elevated p66Shc/ROS-mediated cellular toxicity. Further understanding of the balance between antioxidant HO-1 and prooxidant protein p66Shc is vital in determining the progression of PCa to the CR phenotype. Thus, there is the potential of HO-1 and p66Shc as therapeutic targets and/or biomarkers to be utilized for CR PCa, and thus reduce deaths from this lethal disease. Further analysis is still needed to elucidate the relationship between HO-1, p66Shc, and ROS in PCa tumorigenicity for improving therapy.

Supplementary Material

Refer to Web version on PubMed Central for supplementary material.

Acknowledgments

This study was supported in part by awards of the National Institutes of Health [CA88184, CA230950, CA233664], the Nebraska Redox Biology Center, the University of Nebraska Food for Health Grant, the University of Nebraska Advanced Microscopy Core Facility, the Fred and Pamela Buffet Cancer Center Support Grant [P30CA036727], the UNMC Bridge Fund, the UNMC Cancer Biology Training Grant [T32CA009476], the UNMC Fellowship, and the Purdue Pharma Scholars Award at UNMC. We thank Dr. Melissa Teoh-Fitzgerald for the NBT and Keap1 antibody. We also thank Ms. Fen-Fen Lin for help establish LNCaP-AI and MDA PCa 2b-AI cells as well as p66Shc stable subclones in LNCaP-AS cells.

Abbreviations

Ab	Antibody
ADT	Androgen Deprivation Therapy
AR	Androgen Receptor
AI	Androgen-Independent
AS	Androgen-Sensitive
cFBS	Charcoal/Dextran-treated FBS
CR	Castration-Resistant
ECL	Enhanced Chemiluminescence
FBS	Fetal Bovine Serum
HO-1	Heme Oxygenase-1
H_2O_2	Hydrogen Peroxide
NAC	N-acetyl Cysteine
NBT	Nitro-blue tetrazolium

NOX	NADPH Oxidase
PBS	Phosphate Buffered Saline
PCa	Prostate Cancer
PSA	Prostate Specific Antigen
PO-1	Peroxy Orange-1
PTP	Protein Tyrosine Phosphatase
ROS	Reactive Oxygen Species
RNS	Reactive Nitrogen Species
RTK	Receptor Tyrosine Kinase
Shc	Src homology-collagen homologue
SOD	Superoxide Dismutase
SR	Steroid-Reduced
TBS	Tris-buffered Saline
ZnPPIX	zinc protoporphyrin IX
8-OHG	8-Hydroxyguanine

References

1. Siegel RL, Miller KD, Fuchs HE, Jemal A (2022) Cancer Statistics, 2022. CA: A Cancer Journal for Clinicians 72(1):7–33. [PubMed: 35020204]
2. Seruga B, Ocana A, Tannock IF (2012) Drug resistance in metastatic castration-resistant prostate cancer. Nature Reviews Clin. Onc 8:12–23.
3. Dillard PR, Lin MF, Khan SA (2008) Androgen-independent prostate cancer cells acquire the complete steroidogenic potential of synthesizing testosterone from cholesterol. Mol.Cell Endocrinol 295: 115–120. [PubMed: 18782595]
4. Miller DR, Ingersoll MA, Teply BA, Lin MF (2021) Targeting treatment options for castration-resistant prostate caner. Am J Clin Exp Urol 9(1): 101–120. [PubMed: 33816699]
5. Tannock IF, de Wit R, Berry WR, Horti J, Pluzanska A, Chi KN, Oudard S, Theodore C, James ND, Turesson I, Rosenthal MA, Eisenberger MA (2004) Docetaxel plus prednisone or mitoxantrone plus prednisone for advanced prostate cancer. N Engl J Med 351: 1502–1512. [PubMed: 15470213]
6. Sartor O, Gillessen S (2014) Treatment sequencing in metastatic castrate-resistant prostate cancer. Asian J Androl. 16(3): 426–431. [PubMed: 24675654]
7. Kruk J, Aboul-Enein H (2017) Reactive oxygen and nitrogen species in carcinogenesis: implications of oxidative stress on the progression and development of several cancer types. Mini Reviews in Medicinal Chemistry 17(11): 904–919. [PubMed: 28245782]
8. Oh B, Figtree G, Costa D, Eade T, Hruby G, Lim S, Elfiky A, Martine N, Rosenthal D, Clarke S, Back M (2016) Oxidative stress in prostate cancer patients: a systematic review of case control studies. Prostate Int. 4(3): 71–87. [PubMed: 27689064]
9. Miyake H, Hara I, Kamidono S, Eto H (2004) Oxidative DNA damage in patients with prostate cancer and its response to treatment. J. Urol 171(4): 1533–1536. [PubMed: 15017214]

10. Kumar B, Koul S, Khandrika L, Meacham RB, Koul HK (2008) Oxidative stress is inherent in prostate cancer cells and is required for aggressive phenotype. Cancer Res 68: 1777–1785. [PubMed: 18339858]
11. Veeramani S, Chou YW, Lin FC, Muniyan S, Lin FF, Kumar S, Xie Y, Lele SM, Tu Y, Lin MF (2012) Reactive oxygen species (ROS) by p66shc longevity protein mediate non-genomic androgen action via tyrosine phosphorylation signaling to enhance tumorigenicity of prostate cancer cells. Free Radic Biol Med 53(1):95–108. [PubMed: 22561705]
12. Ingersoll MA, Chou YW, Lin JS, Yuan TC, Miller DR, Xie Y, Tu Y, Oberley-Deegan RE, Batra SK, Lin MF (2018) p66Shc regulates migration of castration-resistant prostate cancer cells. Cell Signal 46: 1–14. [PubMed: 29462661]
13. Miller DR, Ingersoll MA, Chatterjee A, Baker B, Shrishimal S, Kosmacek EA, Zhu Y, Cheng PW, Oberley-Deegan RE, Lin MF (2019) p66Shc protein through a redox mechanism enhances the progression of prostate cancer cells towards castration-resistance. Free Radic Biol Med 139: 24–34. [PubMed: 31100478]
14. Khandrika L, Kumar B, Koul S, Maroni P, Koul HK (2009) Role of oxidative stress in prostate cancer. Cancer Lett. 282(2): 125–136. [PubMed: 19185987]
15. Ripple MO, Henry WF, Rago RP, and Wilding G (1997). Prooxidant–antioxidant shift induced by androgen treatment of human prostate carcinoma cells. J Natl Cancer Inst 89:40–8. [PubMed: 8978405]
16. Basu HS, Wilganowski N, Robertson S, Reuben JM, Cohen EN, Zurita A, Ramachandran S, Xian LC, Titus M, Wilding G (2021) Prostate cancer cells survive anti-androgen and mitochondrial metabolic inhibitors by modulating glycolysis and mitochondrial metabolic activities. The Prostate 81(12): 799–811. [PubMed: 34170017]
17. Veeramani S, Yuan TC, Lin FF, Lin MF (2008) Mitochondrial redox signaling by p66Shc is involved in regulating androgenic growth stimulation of human prostate cancer cells. Oncogene 27(37): 5057–5068. [PubMed: 18504439]
18. Migliaccia E, Giorgio M, Mele S, Pelicci G, Reboldi P, Pandolfi PP, Lanfrancone L, Pelicci PG (1999) The p66Shc adaptor protein controls oxidative stress response and life span in mammals. Nature 402: 309–313. [PubMed: 10580504]
19. Pellegrini M, Pacini S, Baldari CT (2005) p66SHC: the apoptotic side of Shc proteins. Apoptosis 10: 13–18. [PubMed: 15711918]
20. Alam SM, Rajendran M, Ouyang S, Veeramani S, Zhang L, Lin MF (2009) A novel role of Shc adaptor proteins in steroid hormone-regulated cancers. Endocr Relat Cancer 16(1): 1–16 [PubMed: 19001530]
21. Bhat SS, Anand D, Khanday FA (2015) p66Shc as a switch in bringing about contrasting responses in cell growth: implications on cell proliferation and apoptosis. Mol Cancer 14:75. [PubMed: 25879429]
22. Rajendran M, Thomes P, Zhang L, Veeramani S, Lin MF (2010) p66Shc- a longevity redox protein in human prostate cancer progression and metastasis. Cancer Met Rev 29: 207–222.
23. Lee MS, Igawa T, Chen SJ, Van Bemmel D, Lin JS, Lin FF, Johansson SL, Christmas JK, Lin MF (2004) p66Shc protein is upregulated by steroid hormones in hormone-sensitive cancer cells and in primary prostate carcinomas. Int J Cancer 108(5): 672–678. [PubMed: 14696093]
24. Kumar S, Kumar S, Rajendran M, Alam SM, Lin FF, Cheng PW, Lin MF (2011) Steroids up-regulate p66Shc longevity protein in growth regulation by inhibiting its ubiquitination. PLoS One 6(1): e15942. [PubMed: 21264241]
25. Veeramani S, Igawa T, Yuan TC, Lin FF, Lee MS, Lin JS, Johansson SL, Lin MF (2005) Expression of p66Shc protein correlates with proliferation of human prostate cancer cells. Oncogene 24: 7203–7212. [PubMed: 16170380]
26. Gueron G, Giudice J, Valacco P, Paez A, Elguero B, Toscani M, Jaworski F, Leskow FC, Cotignola J, Marti M, Binaghi M, Navone N, Vazquez E (2014) Heme-oxygenase-1 implications in cell morphology and the adhesive behavior of prostate cancer cells. Oncotarget. 5(12): 4087–4102. [PubMed: 24961479]
27. Ma MW, Wang J, Dhandapani KM, Brann DW (2018) Deletion of NADPH oxidase 4 reduces severity of traumatic brain injury. Free Rad. Biol. Med 117: 66–75. [PubMed: 29391196]

28. Ryter SW, Alam J, Choi AMK (2006) Heme Oxygenase-1/carbon monoxide: from basic science to therapeutic applications. Physiol Rev 86:583–650. [PubMed: 16601269]
29. Nitti M, Piras S, Marinari UM, Moretta L, Pronzato MA, Furfaro AL (2017) HO-1 induction in cancer progression: a matter of cell adaption. Antioxidants (Basel) 6(2): 29. [PubMed: 28475131]
30. Maines MD, Abrahamsson PA (1996) Expression of heme oxygenase-1 (HSP32) in human prostate: normal, hyperplastic, and tumor tissue distribution. Urol 47(5): 727–733. [PubMed: 8650873]
31. Alaoui-Jamali MA, Bismar TA, Gupta A, Szarek WA, Su J, Song W, Xu Y, Xu B, Liu G, Vlahakis JZ, Roman G, Jiao J, Schipper HM (2009) A novel experimental heme oxygenase-1-targeted therapy for hormone refractory prostate cancer. Cancer Res 69(20): 8017–8024. [PubMed: 19808972]
32. Sacca P, Meiss R, Casas G, Mazza O, Calvo JC, Navone N, Vazquez E (2007) Nuclear translocation of haeme oxygenase-1 is associated to prostate cancer. Br J Cancer 97(12):1683–1689. [PubMed: 18026199]
33. Li Y, Su J, DingZhang X, Zhang J, Yoshimoto M, Liu S, Bijian K, Gupta A, Squire JA, Alaoui-Jamali MA, Bismar TA (2011) PTEN deletion and heme oxygenase-1 overexpression cooperate in prostate cancer progression and are associated with adverse clinical outcomes. J Pathol 224(1): 90–100. [PubMed: 21381033]
34. Lin MF, Meng TC, Rao PS, Chang CS, Schonthal AH, Lin FF (1998) Expression of human prostatic acid phosphatase correlates with androgen-stimulated cell proliferation in prostate cancer cell lines. J. Biol. Chem 273: 5939–5947. [PubMed: 9488733]
35. Lin MF, Lee MS, Zhou XW, Andressen JC, Meng TC, Johansson SL, West WW, Taylor RJ, Anderson JR, Lin FF (2001) Decreased expression of cellular prostatic acid phosphatase increases tumorigenicity of human prostate cancer cells. J. Urol 166z: 1943–1950.
36. Igawa T, Lin FF, Lee MS, Karan D, Batra SK, Lin MF (2002) Establishment and characterization of androgen-independent human prostate cancer LNCaP cell model. Prostate 50(4): 222–235. [PubMed: 11870800]
37. Chen SJ, Karan D, Johansson SL, Lin FF, Zeckser J, Singh AP, Batra SK, Lin MF (2007) Prostate-derived factor as a paracrine and autocrine factor for the proliferation of androgen receptor-positive human prostate cancer cells. Prostate 67(5): 557–571. [PubMed: 17221842]
38. Miller DM, Ingersoll MA, Chou YW, Wakefield CB, Tu Y, Lin FF, Chaney WG, Lin MF (2017) Anti-androgen abiraterone acetate improves the therapeutic efficacy of statins on castration-resistant prostate cancer cells. J. Oncol. Res. Ther 3: JONT–139. DOI: 10.29011/2574-710X.000039
39. Ingersoll MA, Miller DR, Martinez O, Wakefield CB, Hsieh KC, Kao CL, Chen HT, Batra SK, and Lin MF (2016) Statin-Related Molecules as Therapeutic Agents for Castration-Resistant Prostate Cancer. Cancer Letters (383): 94–105
40. Miller DR, Tzeng CC, Farmer T, Keller ET, Caplan S, Chen YS, Chen YL, Lin MF (2018) Novel CIL-102 derivatives as potential therapeutic agents for docetaxel-resistance prostate cancer. Cancer Lett 436: 96–108. [PubMed: 30077739]
41. Giorgio M, Migliaccio E, Orsini F, Paolucci D, Moroni M, Contursi C, Pelliccia G, Luzi L, Minucci S, Marcaccio M, Pinton P, Rizzuto R, Bernardi P, Paolucci F, Pelicci PG (2005) Electron transfer between cytochrome c and p66Shc generates reactive oxygen species that trigger mitochondrial apoptosis. Cell 122(2): 221–233. [PubMed: 16051147]
42. Perrini S, Tortosa F, Natalicchio A, Pacelli C, Cignarelli A, Palmieri VO, Caccioppoli C, De Stefano F, Porro S, Leonardini A, Ficarella R, De Fazio M, Cocco T, Puglisi F, Laviola L, Palasciano G, Giorgino F (2015) The $p66^{Shc}$ protein controls redox signaling and oxidation-dependent DNA damage in human liver cells. Am. J. Physiol. Gastrointest. Liver Physiol 309: G826–G840. [PubMed: 26336926]
43. Aruny I, Hall S, Faisal A, Dixit M (2017) Nicotine exposure augments renal toxicity of 5-aza-cytidine through p66Shc: prevention by resveratrol. Anticancer Res. 37(8) 4075–4079. [PubMed: 28739690]
44. Burdon RH (1995) Superoxide and hydrogen peroxide in relation to mammalian cell proliferation. Free Rad. Biol. Med 18(4): 775–794. [PubMed: 7750801]

45. Miyazawa M, Tsuji Y (2014) Evidence for a novel antioxidant function and isoform-specific regulation of the human p66Shc gene. Mol. Biol. Cell 25:2116–2127. [PubMed: 24807908]

46. Paez AV, Pallavicini C, Schuster F, Valacco MP, Guidice J, Ortiz EG, Anselmino N, Labanca E, Binaghi M, Salierno M, Marti MA, Cotignola JH, Woloszynska-Read A, Bruno L, Levi V, Navone N, Vazquez ES, Gueron G (2016) Heme oxygenase-1 in the forefront of a multi-molecular network that governs cell-cell contacts and filopodia-induced zippering in prostate cancer. Cell Death Dis 7(12): e2570. [PubMed: 28032857]

47. Shang FT, Hui LL, An XS, Zhang XC, Gui SGm Kui Z (2015) ZnPPIX inhibits peritoneal metastasis of gastric cancer via its antiangiogenic activity. Biomedicine & Pharmacotherapy 71: 240–246. [PubMed: 25960243]

48. Hirai K, Sasahira T, Ohmori H, Fujii K, Kuniyasu H (2007) Inhibition of heme oxygenase-1 by zinc protoporphyrin IX reduces tumor growth of LL/2 lung cancer in C57BL mice. Int. J. Cancer 120(3): 500–505. [PubMed: 17066448]

49. Han L, Jiang J, Ma Q, Wu Z, Wang Z (2018) The inhibition of heme oxygenase-1 enhances the chemosensitivity and suppresses the proliferation of pancreatic cancer cells through the SSH signaling pathway. Int. J. Oncol 52(6): 2101–2109. [PubMed: 29620188]

50. Li Q, Xia T, Yang G, Yang H, Zhang J (2022) Zinc protoporphyrin IX improves the sensitivity of colorectal cancer cells to paclitaxel by inactivating AKT/mTOR pathway via HO-1. Trop. J. Pharm. Res 21(1): 61–66.

51. Fang J, Sawa T, Akaike T, Akuta T, Sahoo SK, Khaled G, Hamada A, Maeda H (2003) In vivo antitumor activity of pegylated zinc protoporphyrin: targeted inhibition of heme oxygenase in solid tumor. Cancer Res. 63:3567–3574. [PubMed: 12839943]

52. Chuang TD, Chen SJ, Lin FF, Veeramani S, Kumar S, Batra SK, Tu Y, Lin MF (2010) Human prostatic acid phosphatase, an authentic tyrosine phosphatase, dephosphorylates ErbB-2 and regulates prostate cancer cell growth. J. Biol. Chem 285(31): 23508–23606.

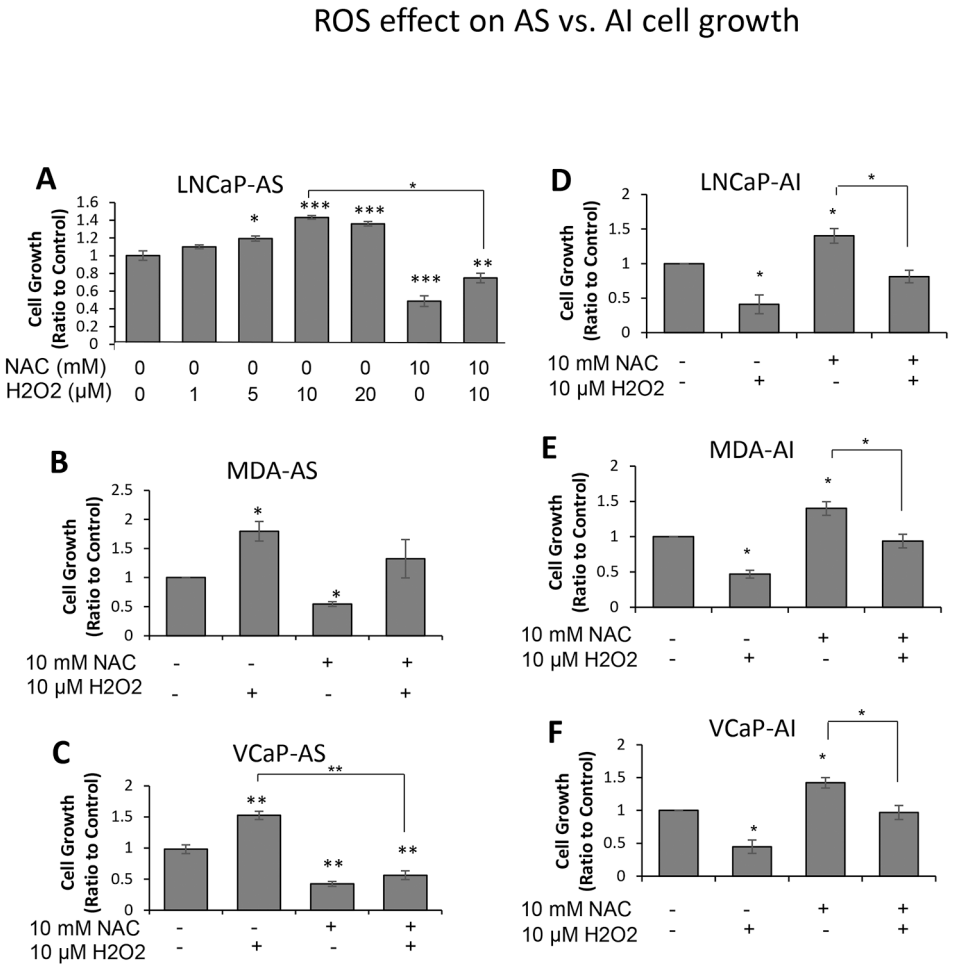

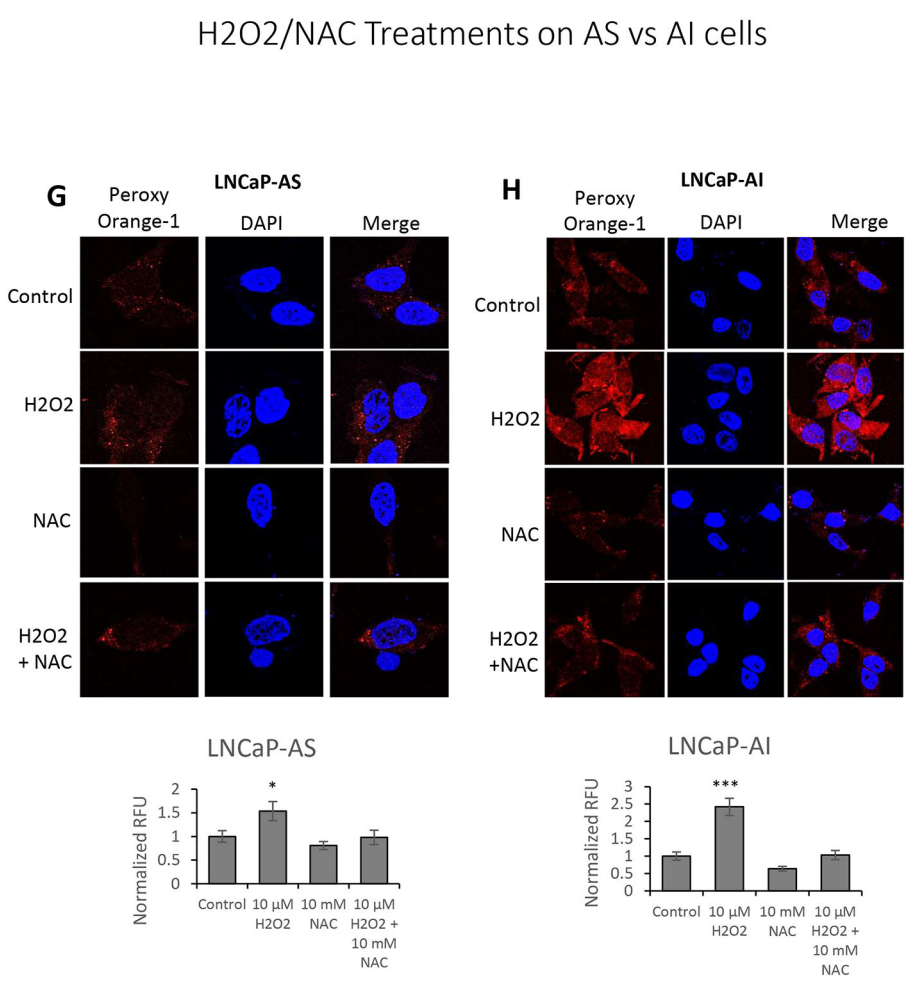

Figure 1. Effects of ROS on AS vs. AI PCa Cell Growth

In Trypan Blue Exclusion Assay, PCa cells, including LNCaP-AS (**A**), MDA PCa2b-AS (**B**), VCaP-AS (**C**), LNCaP-AI (**D**), MDA PCa2b-AI (**E**) and VCaP-AI (**F**) cells, were each plated at 2 x 10^4 cells per well for 72 hours. Cells were treated with 0-20 μM H_2O_2 for LNCaP-AS cells (**A**) and 10 μM H_2O_2 for other cells (**B-F**) plus 10 mM NAC (**A-F**) for 72 hours before cells were harvested and counted via trypan blue exclusion dye. Results presented are mean ± SE. n=3x3. *p<0.05, **p<0.005, ***p<0.0005.

(**G**) LNCaP-AS vs (**H**) LNCaP-AI cells were plated at 5x 10^4 cells per well in 12-well plates for 48 hours. Cells were treated with 10 μM H_2O_2 and/or 10 mM NAC for 24 hours. H_2O_2 levels were labeled with Peroxy Orange-1 fluorescence indicator for 1 hour before the reaction was quenched. DAPI was utilized to stain the nucleus. Fluorescence was visualized via a confocal microscope. Color adjustment was applied equally in all images shown. The data shown is a representative of three sets of independent experiments upon which 20 cells were quantified, and similar results were obtained. n=3. *p<0.05, **p<0.005.

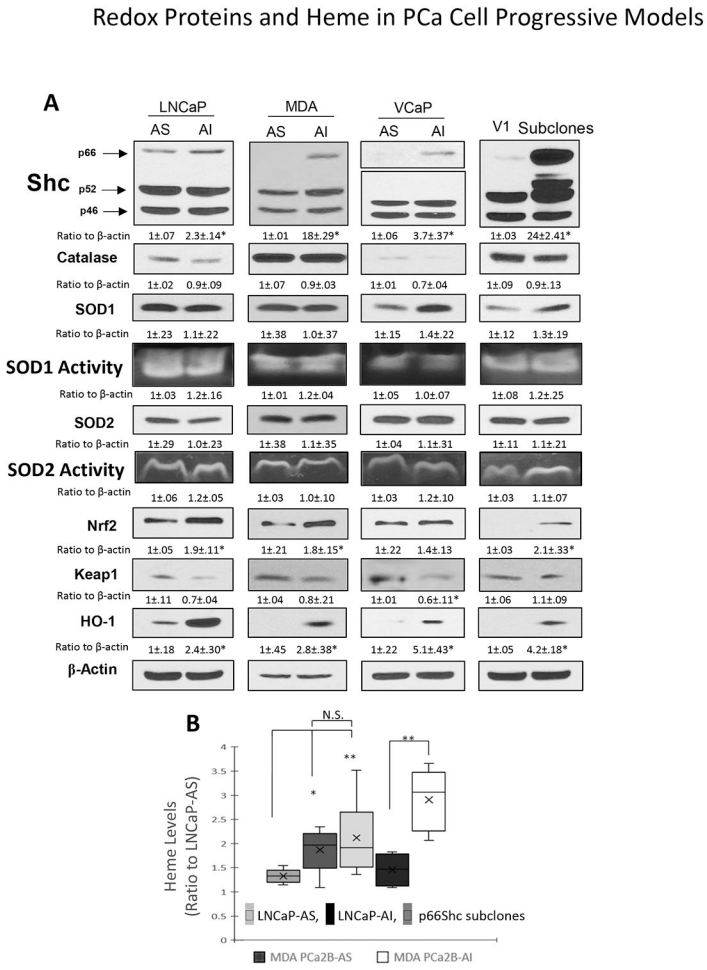

Figure 2. Redox Proteins and Heme Levels in LNCaP, MDA PCa2b and VCaP PCa Cell Progression Models and p66Shc Subclones.

(**A**) Immunoblot analyses of LNCaP, MDA PCa2b, and VCaP cell progression models as well as p66Shc subclones. LNCaP, MDA PCa2b, VCaP, and p66Shc subclone cells were plated in T75 flasks at 1.5 x 10^5, 4 x 10^5, and 4 x 10^5, 3 x 10^5 cells per flask in FBS medium for 72 hours. Cells were harvested via scrapping and lysed. Total cell lysates were analyzed by SDS gels for Shc, Catalase, SOD1, SOD2, NFκB, Nrf2, Keap1, p62, and HO-1. The arrow pointed the position of p66Shc, and p66Shc in VCaP cells was shown upon prolonged exposure. β-actin protein level was used as a loading control. The data shown is a representative of three sets of independent experiments, and similar results were obtained. n=3. To semi-quantify the ratio, the intensities of bands in autoradiograms were analyzed by Image-J program and then normalized to β-actin.

For the SOD Activity Assay, upon harvesting via scrapping, cells were lysed in SDS-free lysis buffer. Cells were then run on a 10% native gel before being subjected to NBT for 20 minutes at room temperature in the dark, then incubated on a light box with riboflavin-5-phosphate for 20 minutes. Gels were washed until the background turned purple in color. n=3.

(**B**) The heme levels of LNCaP-AS vs. -AI cells plus p66Shc subclones and MDAPCa2b-AS vs. -AI cells were sent for metabolomic analyses by Metabolon Inc., Durham, NC. Results shown are the mean ± ranges of 5 samples of each cell line. N=5x1. *p<0.05, **p<0.005

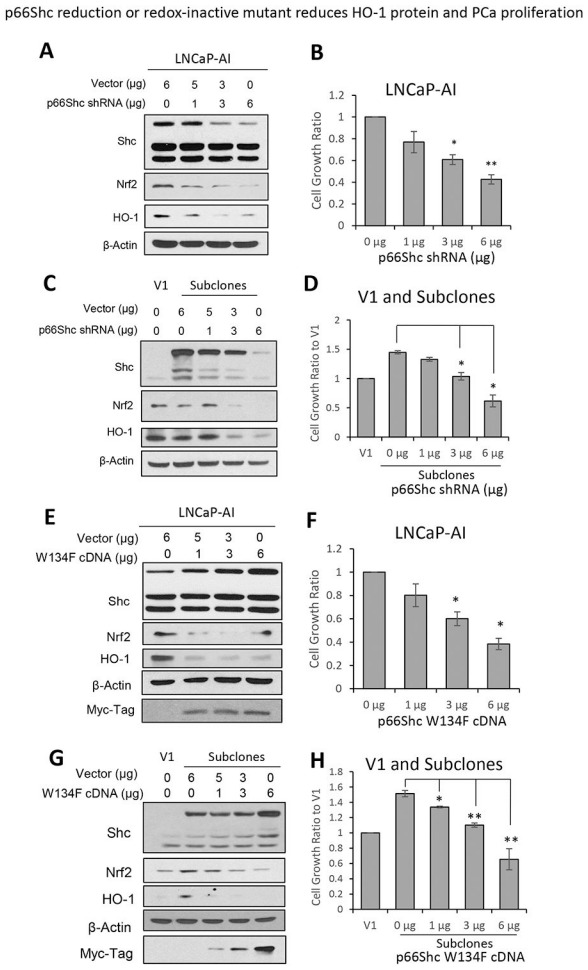

Figure 3. Decreased p66Shc Protein or Activity Reduces HO-1 Protein and PCa Cell Growth.

LNCaP-AI, V1, and p66Shc subclones were plated at 1.5 x 10^5 cells per 100mm petri dish in regular medium containing FBS for 72 hours before being transfected with 0-6 μg of p66Shc shRNA (A-D) or W134F redox-inactive p66Shc cDNA (E-H). Control cells were transfected with vector alone plasmid.

(**A, C, E, G**) 72 hours post-transfection, cells were harvested via scrapping and lysed. Total cell lysates were analyzed for Shc, Nrf2, and HO-1. β-Actin protein level was used as a loading control. Myc-Tag was also analyzed for W134F cDNA transfection. The data shown is a representative of three sets of independent experiments, and similar results were obtained. n=3.

(**B, D, F, H**) p66Shc shRNA-transfected or W134F cDNA-transfected LNCaP-AI, V1, and p66Shc subclone cells were plated at 2 x 10^4 cells per 6-well plate in FBS medium for 72 hours. Cells were then harvested via trypsin, and cell number was measured using trypan blue exclusion dye. Results presented are mean ± SE. n=3x3. *$p<0.05$, **$p<0.005$.

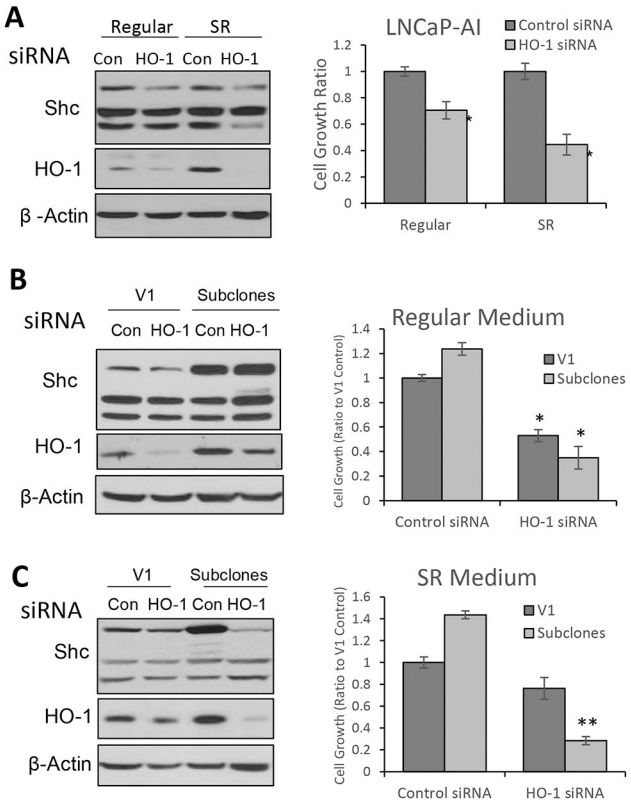

Figure 4. Knockdown of HO-1 Reduces p66Shc and PCa Cell Proliferation.

LNCaP-AI (**A**) and p66Shc subclones (**B** and **C**) cells were plated in FBS medium for 24 hours, then transfected with Control or HO-1 siRNA. Cells were allowed to grow for 72 hours in FBS or SR medium and then harvested via trypsinization. Cell number was counted using trypan blue exclusion dye. Cells were then lysed, and total cell lysates were analyzed for Shc and HO-1. β-Actin protein level was used as a loading control. Results presented are mean ± SE. n=3x3. *p<0.05, **p<0.005.

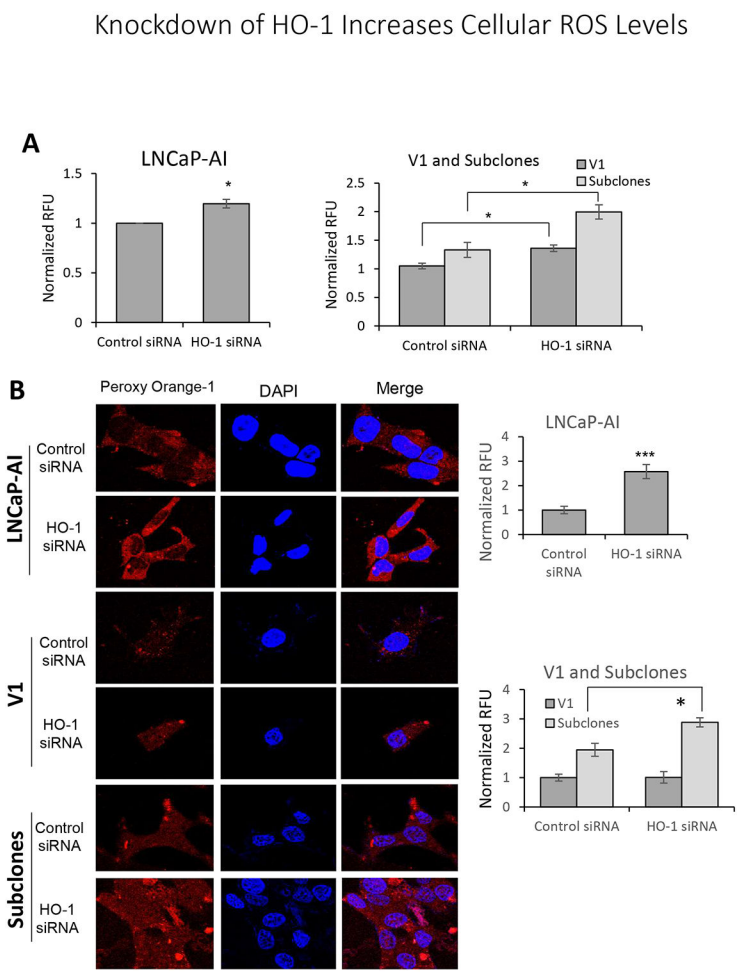

Figure 5. Knockdown of HO-1 Increases the Cellular Oxidative Environment in AI PCa Cells.

(**A**) LNCaP-AI, V1 and p66Shc subclone cells were plated in FBS medium for 24 hours, then transfected with Control or HO-1 siRNA. Cells were allowed to grow for 72 hours in FBS medium and then harvested via trypsinization. Cells were stained with 20 μM DCF-DA for 30 minutes in the dark and subjected to flow cytometry analysis. The data shown is a representative of three sets of independent experiments, and similar results were obtained. n=3. *p<0.05.

(**B**) LNCaP-AI, V1 and p66Shc subclone cells were plated at 5x 10^4 cells per well in 12-well plates for 24 hours. Cells were then transfected with Control or HO-1 siRNA for 48 hours. Cellular peroxide levels were detected upon incubation of the cells with Peroxy Orange-1 (PO-1) for 1 hour. DAPI was utilized to stain the nucleus. Fluorescence was visualized via confocal microscopy. Color adjustment was applied equally in all images shown. The data shown is a representative of three sets of independent experiments, and similar results were obtained. n=3. *p<0.05, **p<0.005, ***p<0.0005.

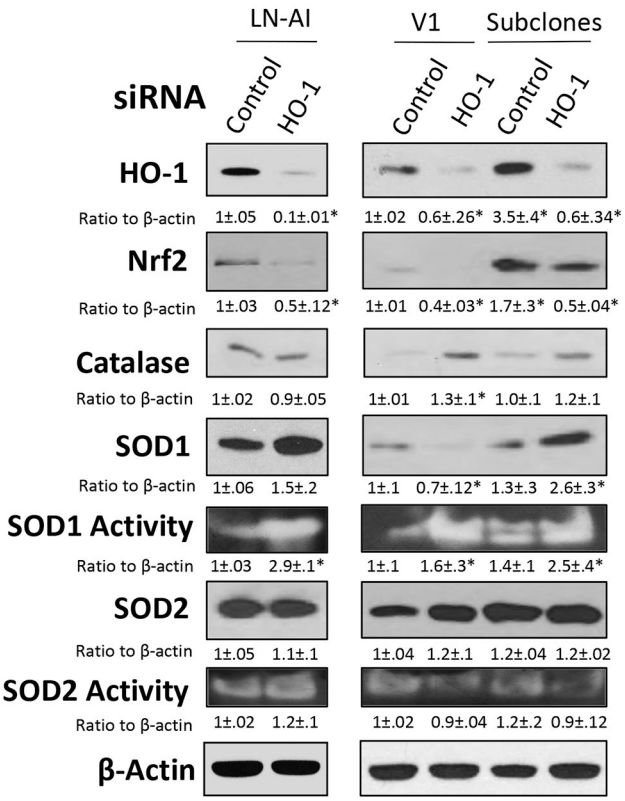

Figure 6. SOD1 activities in HO-1-knockdown AI PCa Cells.

Altered redox proteins in LNCaP-AI and p66Shc subclones transfected with Control or HO-1 siRNA were analyzed by immunoblotting. LNCaP-AI and p66Shc subclones cells were plated in T75 flasks at 1.5 x 10^5 cells per flask in FBS medium for 72 hours then transfected with Control or HO-1 siRNA. Cells were allowed to grow for 72 hours in regular medium containing FBS, then harvested via scrapping and lysed. Total cell lysates were analyzed for Catalase, SOD1, SOD2, NFκB, Nrf2, and HO-1. β-Actin protein level was used as a loading control. The data shown is a representative of three sets of independent experiments, and similar results were obtained. n=3.

To analyze the SOD activity, the cell pellets were lysed in SDS-free lysis buffer. Cell lysates were run on a 10% native gel before being subjected to NBT for 20 minutes at room temperature in the dark, then incubated on a light box with riboflavin-5-phosphate for 20 minutes. Gels were washed until the background turned purple in color. n=3.

To semi-quantify the ratio, the intensities of bands in autoradiograms were analyzed by Image-J program and then normalized to β-actin. *$p<0.05$.

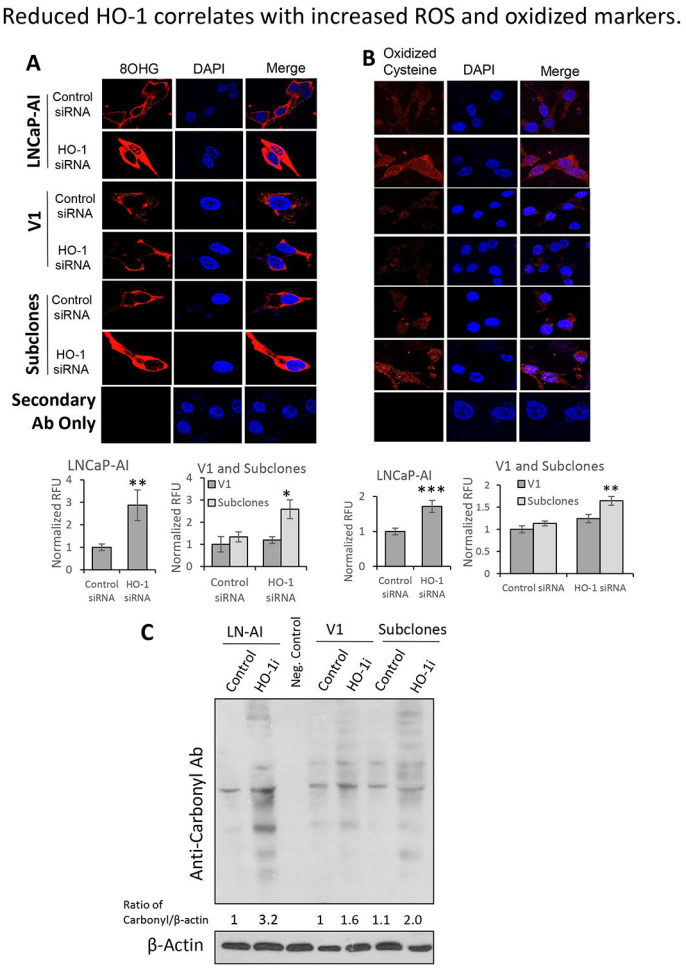

Figure 7. Increased Nucleotide and Protein Oxidation in HO-1-knockdown AI PCa Cells.

(**A&B**) For immunocytochemical analyses on oxidized nucleotides and proteins in HO-1 knockdown cells, LNCaP-AI, V1, and p66Shc subclone cells were plated at 5x 10^4 cells per well in 12-well plates for 24 hours. Cells were then transfected with Control or HO-1 siRNA for 48 hours. Cells were stained with anti-8OHG (**A**) and anti-Oxidized cysteine (**B**) residue primary Abs for 1 hour before staining with a fluorescent-conjugated secondary Ab. DAPI was utilized to stain the nucleus. Fluorescence was visualized via confocal microscopy. Color adjustment was applied equally in all images shown. The data shown is a representative of three sets of independent experiments, and similar results were obtained. n=3. *p<0.05, **p<0.005, ***p<0.0005.

(**C**) Immunoblot analysis of oxidized proteins in HO-1 knockdown cells, experimental cells and control cells were harvested via scrapping and lysed. Total cell lysates were analyzed for carbonylated proteins. β-Actin protein level was used as a loading control. The data shown is a representative of three sets of independent experiments, and similar results were obtained. n=3. To semi-quantify the ratio, the intensities of the major bands in autoradiograms were analyzed by Image-J program and then normalized to β-actin.

HO-1 KD with decreased cell growth and increases apoptosis

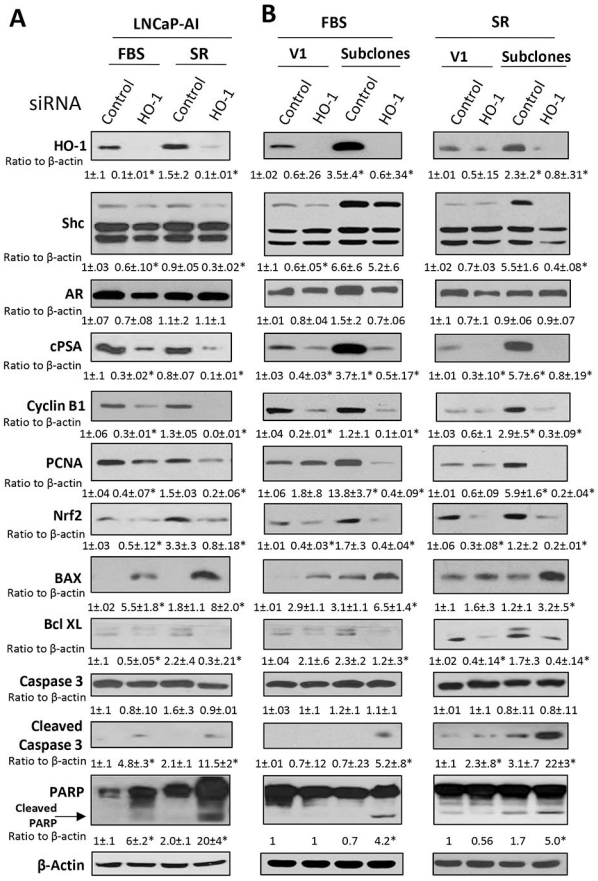

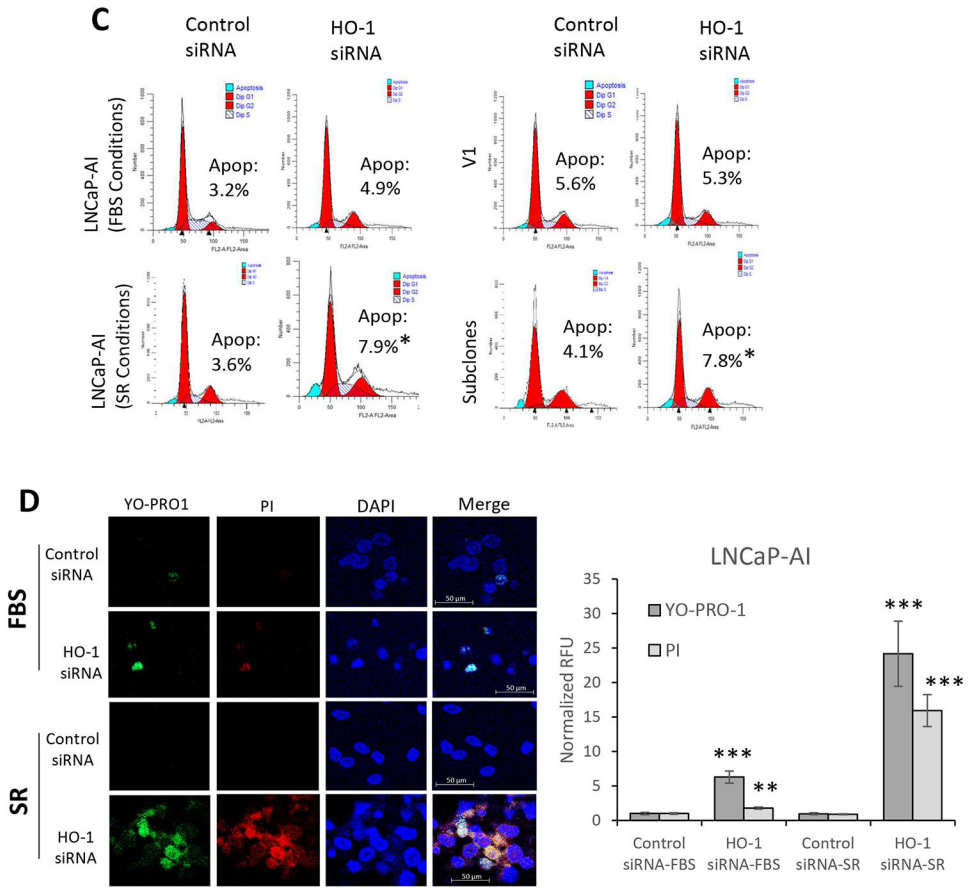

Figure 8. HO-1 Knockdown Correlates with Increased Cell Death Biomarkers in AI PCa Cells under FBS and SR Conditions.

Immunoblot analyses of LNCaP-AI (**A**) and p66Shc subclones (**B**) transfected with Control or HO-1 siRNA. LNCaP-AI and p66Shc subclones cells were plated in T75 flasks at 1.5 x 10^5 cells per flask in FBS medium for 72 hours then transfected with Control or HO-1 siRNA. Cells were allowed to grow for 72 hours in FBS or SR medium, and then harvested via scrapping and lysed. Total cell lysates were analyzed for Shc, AR, cPSA, Cyclin B1, PCNA, Nrf2, HO-1, BAX, BclXL, Caspase 3, and PARP proteins. β-Actin protein level was used as a loading control. The data shown is a representative of three sets of independent experiments, and similar results were obtained. n=3. To semi-quantify the ratio, the intensities of the bands in autoradiograms were analyzed by Image-J program and then normalized to β-actin. The data shown is the mean of results from three sets of independent experiments. n=3. *p<0.05.

(C) Cell Cycle Analyses of LNCaP-AI and p66Shc subclones transfected with Control or HO-1 siRNA. LNCaP-AI and p66Shc subclones cells were plated in T75 flasks at 1.5 x 10^5 cells per flask in FBS medium for 72 hours then transfected with Control or HO-1 siRNA. Cells were allowed to grow for 72 hours in FBS or SR medium and then harvested via trypsinization. Cells were fixed with 70% ethanol for 30 minutes, then washed twice with PBS. Cells were stained with Telford reagent for 2 hours, and then cell cycle was analyzed via flow cytometry. The data shown is a representative of three sets of independent experiments, and similar results were obtained. n=3. *p<0.05.

(**D**) LNCaP-AI cells were plated at 5x 10^4 cells per well in 12-well plates for 24 hours. Cells were then transfected with Control or HO-1 siRNA for 48 hours. Cells were stained with YO-PRO-1 and PI stains for 30 minutes. DAPI was utilized to stain the nucleus. Fluorescence was visualized via confocal microscopy. Color adjustment was applied equally in all images shown. The data shown is a representative of three sets of independent experiments, and similar results were obtained. n=3. **p<0.005, ***p<0.0005.

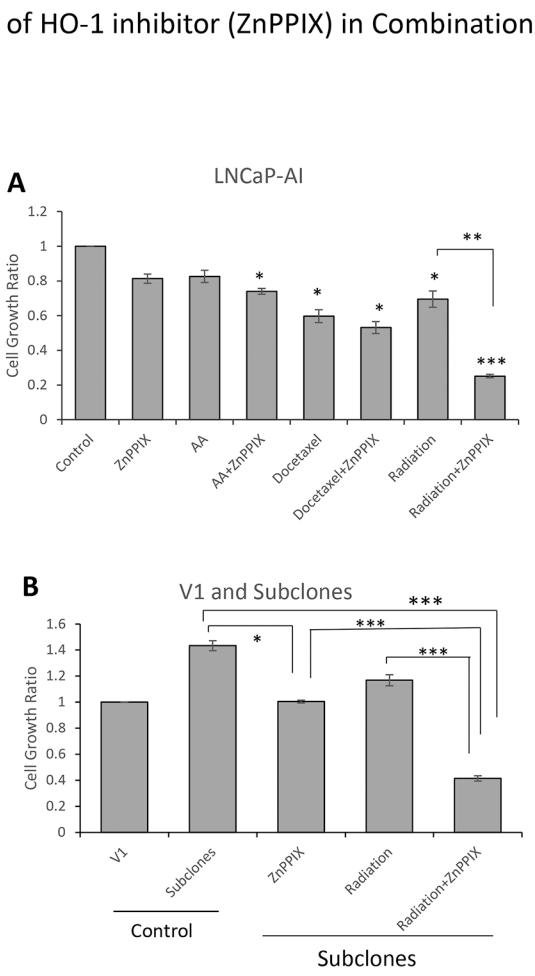

Figure 9. Effect of HO-1 Inhibition on Combination with Standard Treatments for CR PCa.

LNCaP-AI (**A**), V1 and p66Shc subclones (**B**) were plated at 1.5 x 10^5 cells per flask in FBS medium for 72 hours before experiments. Post-transfection, cells were treated with 2 μM of ZnPPIX, radiation (5 Gy), Docetaxel (1 nM), or Abiraterone acetate (5 μM) for 72 hours. Cells were then harvested via trypsinization, and cell number was measured using trypan blue exclusion dye. Results presented are mean ± SE. n=3x3. *p<0.05, **p<0.005, ***p<0.0005.

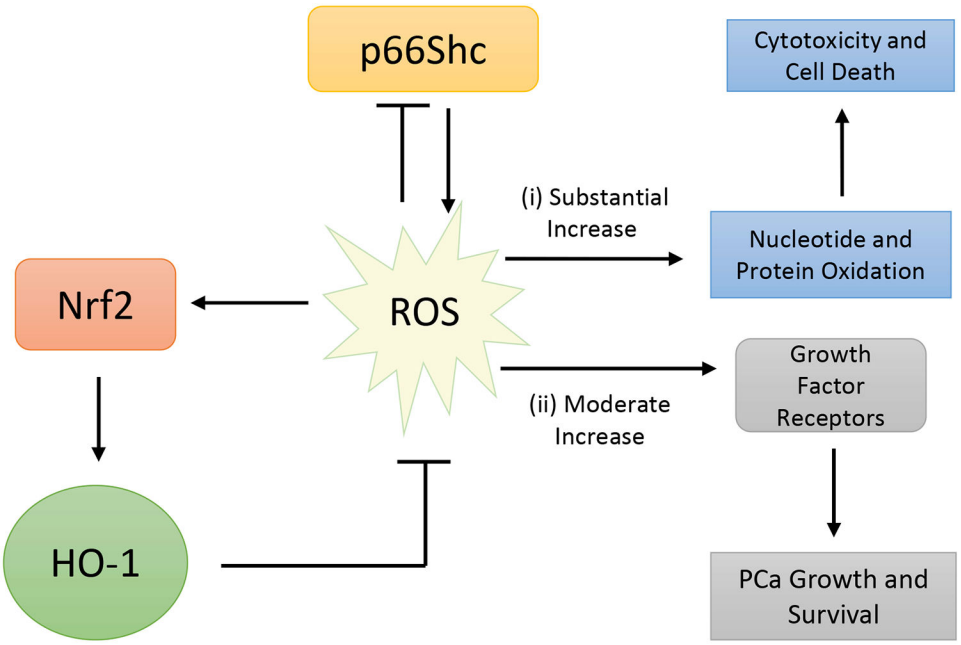

Figure 10. Scheme of Working Hypothesis.

Pro-oxidant protein p66Shc enhances ROS generation via interaction with cytochrome c in the mitochondria or via activation of NADPH oxidase in the cytoplasm. Interestingly, increased ROS can also reduce p66Shc protein levels. Upon increased ROS levels, Nrf2 is activated and promotes transcription of antioxidant enzyme HO-1 to reduce ROS-induced oxidative stress and/or damage. (i) A substantial, excessive increase of ROS leads to cytotoxicity and apoptosis of the cell. (ii) However, a moderate increase in ROS can promote PCa cell growth and survival via oxidation of negative growth regulators, such as protein tyrosine phosphatases.